

# The Successive Wave Decomposition Method Basing On the Harmonic Analysis

## 應用調和函數分析法的疊代式複合波依次拆解法

Yih Nen Jeng (鄭育能)

Professor of Aero. and Astro. Dept., National Cheng-Kung Univ., Taiwan

Z6208016@email.ncku.edu.tw

You-Chi Cheng (鄭又齊)

Engineer, Zu-Soft Company, Taipei, Taiwan

### ABSTRACT

It is proven that the classical Fourier series expansion can not completely capture all information of a real data string. A successive wave decomposition method via the harmonic analysis is proposed. By assuming the amplitude to be changeable for a single sine function, the least squares method is employed to search the minimized error measure function. Since the extreme process is nonlinear, the initial guesses are provided via the Fast Fourier Transform and an iteration procedure is proposed. Starting from the mode with the largest amplitude, dominated modes are decoupled one by one. The spectrum of a single mode with variable amplitude is a scattered band which shows the insufficient information reflected by the classical Fourier spectrum.

**Keywords:** High order harmonic analysis, successive decoupling, variable amplitude.

### 摘 要

本文證明傳統的快速傅式級數無法完美地補捉一般數據串的資訊。本文應用高階的調和函數分析法，發展出疊代式依次拆解複合波法，一次拆解一個波，並允許振幅可隨時間改變。數值測試顯示振幅改變的波會在頻譜圖上造成對應於頻率之主頻旁含有數個小模式的訊息，同時也可證明完美的拆解法需要允許所有的參數都可變。

**關鍵詞：**高階調和函數分析法，疊代式最小平方誤差法，可變振幅法。

### 1. Introduction

Because of the rapid development of computer technique, people can collect many data string simultaneously now. In near future, the nano technology will further increase the number of data strings exponentially. How to analyze these data string automatically becomes an important issue. To the authors' knowledge, the procedure includes data validation to remove anomalies; decompose data

string into smooth non-sinusoidal, pseudo-sinusoidal, and random parts; and wave decomposition. In the classical analysis, the wave decomposition step frequently employs the Fourier series transformation to obtain the spectrum [1,2]. However, all the amplitudes and frequencies (or wavelengths) given by the spectrum are constant. The information about the phase angle is reflected by the real and imaginary part of the spectrum.

Unfortunately, many people do not aware of the necessity of removing the smoothing non-sinusoidal part before employing the transformation and frequently generate a spectrum containing an unknown exponentially decayed part in the low frequency region. Moreover, it is impossible to assure the periodic condition for every mode. Consequently, people can only get qualitative information of the sinusoidal part.

In order to remedy the above mentioned drawbacks, there are two successive methods which work very well. The first method is the matrix pencil method which employs the singular value decomposition to find the local amplitude, wavelength and phase angle [3,4]. The other method is the empirical mode decomposition proposed by Huang et. al. [5,6]. The method employs the cubic spline interpolation to fit the local maximum and minimum points separately to estimate the upper and lower boundaries of a data string. The average of these two boundaries is an estimation of the low frequency part and is refined by an iteration procedure. Finally, the Hilbert transform is employed to estimate the amplitude, wavelength, and phase angle. Although these two method works successfully, the zero order approximation of the matrix pencil method and the unknown numerical part introduced in the step of estimating the upper and lower boundaries point out the necessity of developing a sophisticate high order method.

## 2. Contents

### 2.1 Analysis

Consider a data string of  $(x_i, y_i)$ ,  $i = 0, 1, 2, \dots, n$ , where  $\Delta x_i = x_{i+1} - x_i = \text{constant}$ ,  $x$  denotes time or other independent variable and  $y$  is the dependent variable. The discrete Fourier series expansion expands the data into

$$\begin{aligned} y_i &\approx f(x_i) = \sum_{p=0}^n [A_p \cos \frac{2\pi p i}{n+1} + B_p \sin \frac{2\pi p i}{n+1}] \\ &= \sum_{p=0}^n [A_p \cos \frac{2\pi p x_i}{L} + B_p \sin \frac{2\pi p x_i}{L}] \end{aligned} \quad (1)$$

with the assumption of adding a ghost point  $x_{n+1} = x_n + \Delta x$  and  $y_{n+1} = y_0$ , where  $L = x_{n+1} - x_0$ . In order to employ the discrete Fast Fourier Transform (FFT) algorithm whose number of points equals to  $2^k$  and reduce the error induced by non-periodic boundary condition, a previous work [7] find points where  $y_i \leq 0$ ,  $y_{i+1} \geq 0$  (or  $y_i \geq 0$ ,  $y_{i+1} \leq 0$ ) around two ends, and takes the points where  $y = 0$  in terms of the linear or high order interpolation as new end points. Subsequently, the data is reconstructed to be of points whose number is equal to  $2^k$  via the following monotonic cubic spline interpolation is employed [8].

$$\begin{aligned} y(x) &= c_3(x - x_i)^3 + c_2(x - x_i)^2 + c_1(x - x_i) + c_0, \\ c_0 &= y_i, c_1 = y'_i, \quad s_{i+1/2} = \frac{y_{i+1} - y_i}{x_{i+1} - x_i} \\ c_2 &= \frac{3s_{i+1/2} - 2y'_i - y'_{i+1}}{x_{i+1} - x_i}, \quad c_3 = \frac{y'_i + y'_{i+1} - 2s_{i+1/2}}{(x_{i+1} - x_i)^2}, \end{aligned} \quad (2)$$

with

$$\begin{aligned} y'_i &= \text{sgn}(t_i) \min\left[\frac{1}{2} |p'_{i-1/2} + p'_{i+1/2}|, \max(k |s_i|, \frac{k}{2} |t_i|)\right] \\ p'_{i-1/2} &= s_{i-1/2} + d_{i-1/2}(x_i - x_{i-1}) \\ p'_{i+1/2} &= s_{i+1/2} + d_{i+1/2}(x_i - x_{i+1}) \\ t_i &= \min \text{mod}[p'_{i-1/2}(x_i), p'_{i+1/2}(x_i)] \\ d_{i+1/2} &= \min \text{mod}(d_i, d_{i+1}), \quad d_i = \frac{s_{i+1/2} - s_{i-1/2}}{x_{i+1} - x_{i-1}}, \\ s_i &= \min \text{mod}[s_{i-1/2}, s_{i+1/2}] \end{aligned} \quad (3)$$

where  $k \geq 4$  for smooth data and

$$\begin{aligned} y'_i &= y'_{i+1}, \quad \text{if } |y_{i+1} - 2y_i + y_{i-1}| \leq \varepsilon \\ &\quad \text{or } |y_{i+2} - 2y_{i+1} + y_i| \leq \varepsilon \end{aligned} \quad (4)$$

in which  $\varepsilon$  is an user specified infinitesimal positive constant. After make sure that number of points is of  $2^k$ , the simple FFT algorithm is employed to find the spectrum. For a dominate mode whose mode number is  $j$ , the corresponding wavelength is

estimated as

$$\lambda_j = \frac{x_N - x_0}{j} \quad (5)$$

where  $x_0$  and  $x_N$  are new end points with  $N = 2^k + 1$ . The amplitude estimation is directly read from the spectrum.

In fact, the formula of Eq.(1) is not perfect for a data string which may be in form of

$$y_i = \sum_{p=0}^m \bar{A}_p(x_i) \sin\left(\frac{2\pi f_p(x_i)x_i}{L} + \theta_p(x_i)\right) \quad (6)$$

If  $m \leq n$  and all the amplitudes, frequencies, and phase angles are constants, and if the following equalities are valid

$$\begin{aligned} \bar{A}_p &= \sqrt{A_p^2 + B_p^2}, \quad f_p = p, \\ \theta_p &= \tan^{-1}[B_p / A_p] \end{aligned} \quad (7)$$

Eq.(1) is equal to Eq.(6) exactly. In general, Eq.(1) is not equal to Eq.(6) because all the equalities of Eq.(7) may not be satisfied. In other words, Eq.(7) is a set of constraint rather than a system of resulting formulas. The reason is that, even for the situation of  $f_p$ 's and  $\theta_p$ 's = constants, the resolution of data point may not be sufficient to ensure the following conditions for all modes

$$\begin{aligned} f_p &= p, \quad 0 \leq p \leq n, \quad p \in I \\ m &\leq n, \end{aligned} \quad (8)$$

where  $I$  denotes the integer set.

As noted in Ref.[7], the smooth non-sinusoidal part always introduces undesired low frequency part. For example, Fig.1 is a smooth data string where the periodic condition is obviously violated. Figure 2 is the corresponding spectrum which shows a zigzag and exponentially decayed distribution. So far the method of exactly removing the smooth non-sinusoidal part is still an open problem and all the existing methods are not very popular. Therefore, many people employing the spectral

analysis may not aware of this contamination involving in the spectrum.

## 2.2 Iteration Procedure for Constant Parameters

In order to demonstrate the proposed algorithm, the simplest case is shown firstly. Consider the case that all the amplitudes, frequencies, and phase angles are constant. Following the harmonic analysis, the error measure function is defined as follows.

$$I_p = \sum_{i=0}^n [y_i - A_p \sin\left\{\frac{2\pi f_p x_i}{L} + \theta_p\right\}]^2 \quad (9)$$

Although setting the partial derivatives of the function with respect to parameters  $A_p$ ,  $f_p$ , and  $\theta_p$  will generate the desired approximation in a least squares sense, it is a highly non-linear extreme procedure which may or may not leads to a local minimum rather than the global minimum. Fortunately, both  $A_p$  and  $f_p$  can be estimated as stated in Eq.(5) and the spectrum find from the method of Ref.[7], a searching loop to find the true minimum of  $I_p$  via the following procedure:

1. Estimate  $A_p$  and  $f_p$ .
2. Change  $\theta_p$  to search the minimum  $I_p$ , this step is the inner loop.
3. Use the variation of  $f_p$  as the medium loop and the variation of  $A_p$  as the outer loop, and then search the minimum  $I_p$ .

## 2.3. Variable Amplitude Version

Because this is only but a first study, variations of  $f_p$  and  $\theta_p$  are not considered here. The error measure function is now defined as

$$\begin{aligned} I_p &= \sum_{i=0}^n [y_i - (A_{0,p} + A_{1,p}\bar{x} + A_{2,p}\bar{x}^2 + A_{3,p}\bar{x}^3) \\ &\quad \times \sin\left\{\frac{2\pi f_p x_i}{L} + \theta_p\right\}]^2, \quad \bar{x}_i = x_i - x_c \end{aligned} \quad (10)$$

where  $x_c = (x_0 + x_N)/2$ . The outer loop now can be replaced by the solution of

$$\frac{\partial I_p}{\partial A_{0,p}} = 0, \quad \frac{\partial I_p}{\partial A_{1,p}} = 0, \quad \frac{\partial I_p}{\partial A_{2,p}} = 0, \quad \frac{\partial I_p}{\partial A_{3,p}} = 0 \quad (11)$$

where  $f_p$  and  $\theta_p$  are fixed. Then, the iteration procedure of section 2.2 can be employed.

### 3. Results and Discussions

One of the test data of Ref.[7] is the vertical displacement at the central point of a steel specimen excited by a hammer. A segment of the original data is drawn in Fig.3 and the corresponding spectrum is shown in Fig.4. The low frequency part are nearly vanishing because of the approximation of Ref.[7] does remove most low frequency error. After applying two cycles of the present successive decoupling procedure for constant parameters, the resulting waves are shown in Figs.5 and 6, respectively. The corresponding spectrum of the remaining data is shown in Fig.7. Although the remaining data is somewhat like the white noise, there is still some minor peak around the original mode. This means that the amplitude of the dominate mode may be slightly varied. This example shows the necessity of applying the variable parameter scheme.

The second test case to demonstrate the variable amplitude version of the successive decouple procedure is a tide wave data. The data is shown in Fig.8 which shows that many tide waves with slightly different wavelengths form a beat wave. The remaining wave after applying twelve cycles of the decouple procedure is also shown in the figure. Their corresponding spectrums are shown in Fig.9 where the original data's spectrum shows the wavelength clustering together and the remaining waves still involve many minor waves. The fact of many waves in the remaining part reflects that the version of variable amplitude is still not enough and the decouple procedure should contain variable wavelength and phase angle. All the results of the twelve cycles are listed in Table I

which indicates serious variation of the amplitude. The resulting waves of the first three modes are shown in Figs.10, 11 and 12 which involve serious amplitude variation. The corresponding spectrums of all the decoupled waves are shown in Figs.13 through 16, respectively. From these spectrum distributions, it is clear that every spectrum of each wave is not longer a single peak in the spectrum domain. The variation of amplitude splits the single peak into several minor peaks around the largest peak.

The above discussion shows that the classical FFT cannot provide all information of a data string. Therefore, a new analytical tool to involve variable amplitude, wavelength, and phase angle is necessary. This fact indicates that the direction of present study is positive.

### 4. Conclusions

A new high order harmonic analysis is proposed. An iteration procedure is constructed to overcome the difficulty of highly nonlinearity of the minimizing process. Numerical studies show that the present study is not enough and a still more complete version of the high order harmonic analysis is necessary.

### 5. Acknowledgement

This work is supported by the National Science Council of Taiwan under the grant number NSC-92-2212-E006-077.

### 6. References

1. Brigham, E. O., *The Fast Fourier Transform*, Prentice-Hall Inc. Englewood Cliffs, N. J., 1974, pp.164.
2. P. M. Morse and H. Feshbach, "Methods of Theoretical Physics," New York, McGraw-Hill, vol.2, 1953.
3. Hua, R. and Sarkar, T. K., "Generalized Pencil-of-Function Method for Extracting Poles of an EM System from Its Transient Response," IEEE Trans. Antennas and Propagation, vol.37, no.2, Feb. 1989, pp.229-234.

4. Ruscio, D. D., "On Subspace Identification of Extended Observability Matrix," Proc. Of 36<sup>th</sup> Conf. on Decision & Control., San Diego, Cal. U.S.A., Dec. 1997, Paper no.TA05, pp.1841-1847.
5. N. E. Huang, Z. Shen, and S. R. Long, "A New View of Nonlinear Water Waves: the Hilbert Spectrum," Annual Reviews of Fluid Mechanics, 1999, vol.51, pp.417-457.
6. Huang, N. E., Shen, Z., Long, S. R., Wu, M. C., Shih, H. H., Zheng, Q., Yen, N. C., Tung, C. C. and Liu, H. H., "The Empirical Mode Decomposition and the Hilbert Spectrum for Nonlinear and Non-stationary Time Series Analysis," Proc. Royal Soc. London A, vol. 454, pp.903- 995, 1998.
7. Y. N. Jeng and Y. C. Cheng, "A Simple Strategy to Evaluate the Frequency Spectrum of a Time Series Data with Non-Uniform Intervals", 10-th National Computational Fluid Dynamics Conference of Taiwan, Hua-Lien, 2003, Paper no.A-9, also Transactions of the Aeronautical and Astronautic Society of the Republic of China in press, 2004.
8. Huynh, H. T., "Accurate Monotone Cubic Interpolation," *SIAM J. Number. Anal.* vol.30, no.1, pp57-100, Feb.1993.

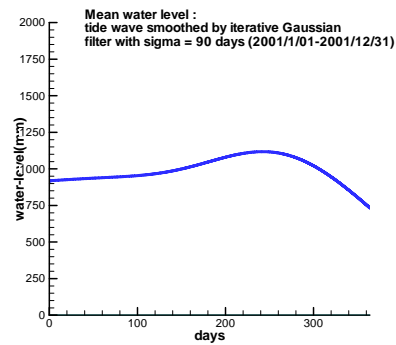


Fig.1 An example of smooth non-sinusoidal data.

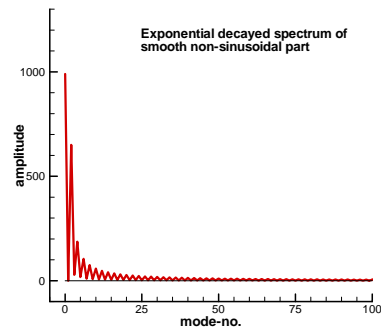


Fig.2 The corresponding spectrum of Fig.1.

**Table I**

$p =$	$\lambda_p$	$\theta_p$	Amp. ( $A_{0,p}, A_{1,p}, A_{2,p}, A_{3,p}$ ) (mm)			
1	0.99647	1.0054	-221.196	-94.405	-365.953	524.710
2	1.07400	.3319	-195.198	32.8721	50.0977	295.263
3	1.12301	.9018	-56.0107	-10.6963	21.2860	84.1467
4	1.02267	.1391	35.1338	-28.6496	151.116	-14.7617
5	0.98073	.7591	11.1557	-62.6774	58.4167	-28.5127
6	1.05974	1.0142	-12.5623	-25.7506	-12.0562	41.2189
7	1.16020	.7727	-16.2968	20.2689	28.1911	-25.2297
8	0.94945	.2070	10.8695	4.8186	2.5490	-4.8910
9	1.01152	.6585	-8.6861	11.5764	-41.2419	24.6887
10	1.61886	1.6189	-1.6873	-36.8529	-9.6339	20.5446
11	1.37352	.1923	-3.8086	-24.1370	-14.2167	-2.9655
12	0.87808	.8605	3.9353	-21.9143	-1.2341	2.1218

\* The phase angle =  $2\pi\theta_p / \lambda_p$ , if  $\theta_p < \lambda_p$ .  
Otherwise it is equal to  $2\pi(\theta_p - \lambda_p) / \lambda_p$

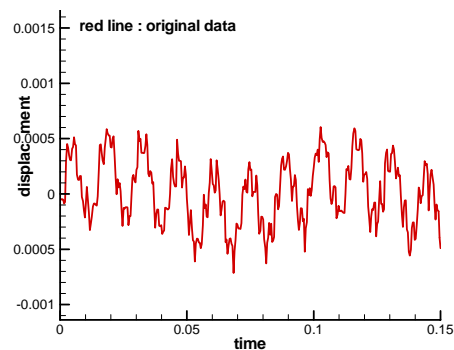


Fig.3 The segment plot of the original data of the vertical displacement.

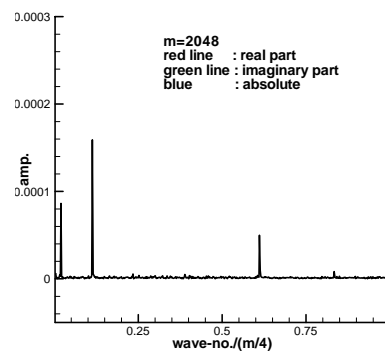


Fig.4 The spectrum of Fig.3 generated by the method of Ref.[7]

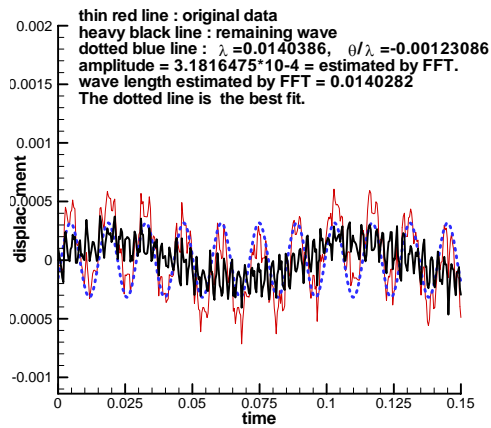


Fig.5 The result of the first cycle decouple: dotted line is the removed mode and heavy line is the remaining wave.

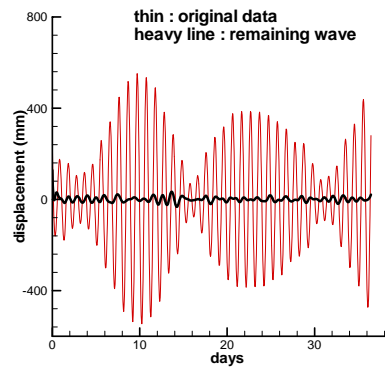


Fig.8 The original data and the remaining wave after 12 cycles of wave removing.

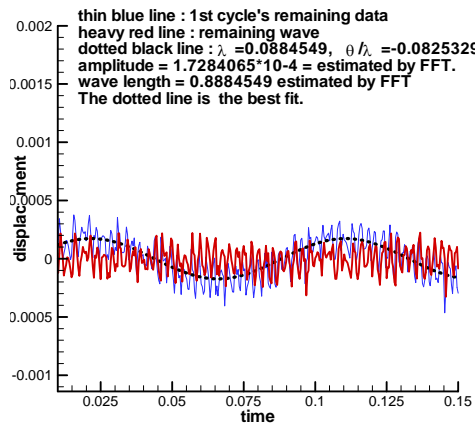


Fig.6 The result of the second cycle of decouple: the thin line is the first cycle's remaining part, the dotted line is the removed wave of the second cycle, and the heavy line is the remaining wave of the second cycle.

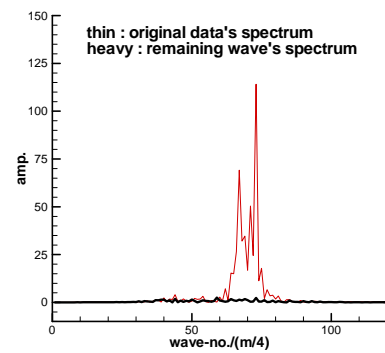


Fig.9 Spectrum of the original data and the final remaining waves

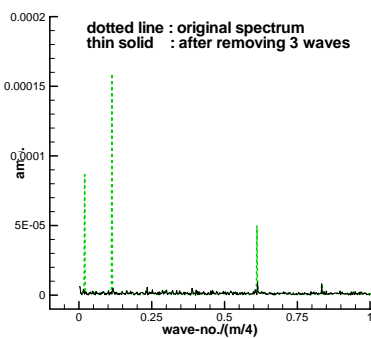


Fig.7 The spectrum of the original data is the dotted line and the remain data's spectrum is solid line.

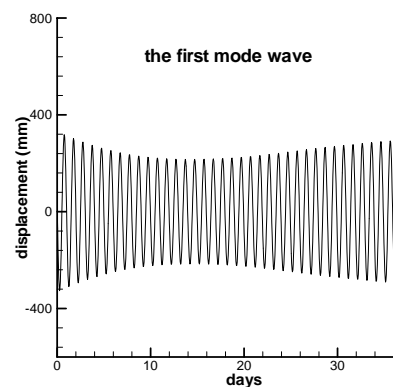


Fig.10 The first mode decoupled from the original data.

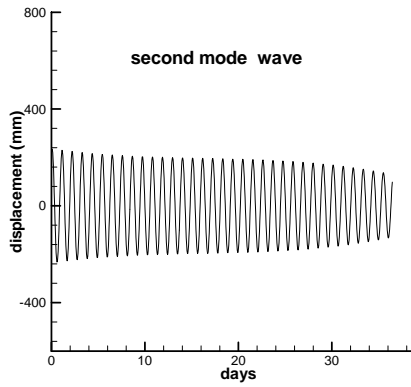


Fig. 11 the second mode decoupled from the data.

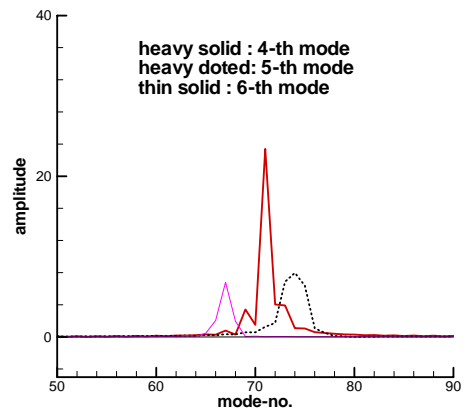


Fig. 14 Spectrum of the second three modes

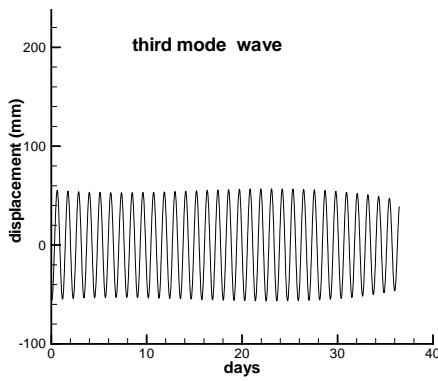


Fig. 12 The third mode decoupled from the data

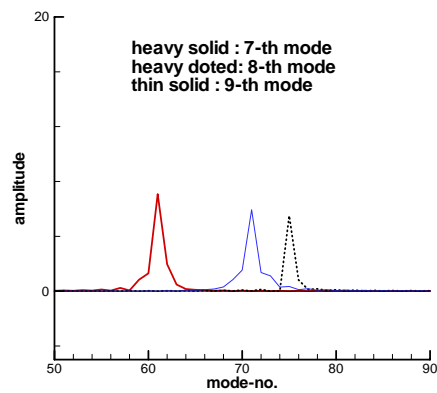


Fig. 15 Spectrum of the third three modes.

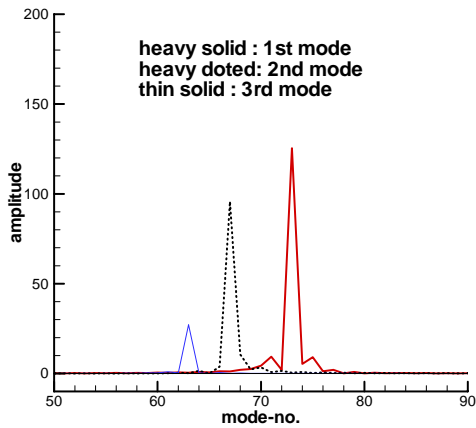


Fig. 13 Spectrum of the first three modes

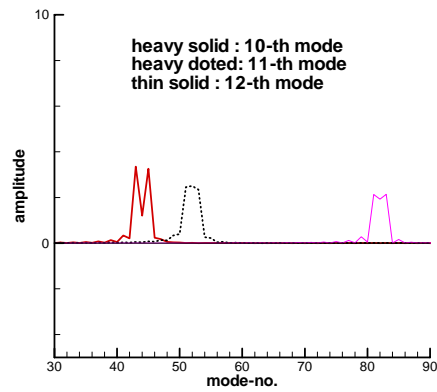


Fig. 16 Spectrum of the fourth three modes.